ISSN:3007-9640 DOI: https://doi.org/10.70114/acmsr.2025.3.1.P56

Hazardous Gas Monitoring Technology for Natural Gas Pipelines Based on GoogLeNet Infrared Spectroscopy

Tao Cui [a] *, Zhifeng Wu, Li Gu, Yanjie Jia and Jiangqiao Lian

[1] PipeChina Group Southwest Pipeline Co., LTD, Sichuan Chengdu, China;

[a] 876930041@qq.com

Abstract. During the natural gas transmission process, the leakage of hazardous gases poses a long-term threat to production. Therefore, an online and intuitive monitoring method is particularly important. Based on research on infrared spectroscopy and deep learning, this study proposes the use of deep learning and infrared spectroscopy to monitor hazardous gases in the natural gas transmission process. The GoogLeNet model is employed to analyze the infrared spectra of hazardous gases in natural gas transmission, and a symmetric point-based GoogLeNet infrared spectroscopy monitoring scheme is proposed.In comparative experiments, considering all performance evaluation metrics, GoogLeNet demonstrates significant advantages in detecting hazardous gases in natural gas transmission. Its mean average precision (mAP) and accuracy outperform other models. Furthermore, after expanding the dataset and retraining the GoogLeNet model, its performance is further improved, ensuring that it meets the fundamental requirements for hazardous gas detection in the natural gas transmission process.

Keywords: Natural gas transmission, Hazardous gas, Infrared spectroscopy, Deep learning.

1. Introduction

During the natural gas transmission process, leaks can lead to the release of hazardous gases. Common hazardous gases include biogas (methane) and methane homologs (ethane, propane, etc.) [1]. According to relevant statistics, approximately 70% to 75% of casualties in natural gas pipeline explosions or fire accidents are caused by carbon monoxide poisoning [2].

Methane (CH_4) is the most common and primary gas in natural gas [3]. It is an asphyxiating and explosive gas. Methane poses the greatest threat to coal mine safety. In underground operations, hazardous gases that primarily contain high concentrations of methane are commonly referred to as "gas" [4].

As the safety level of natural gas transmission continues to improve, the widespread application of hazardous gas monitoring systems has led to the gradual refinement of detection methods. A comprehensive monitoring system integrating both manual and automated monitoring technologies has been established throughout the transmission process.

Manual detection methods typically rely on sampling and analysis, which are both hazardous and time-consuming. However, real-time online monitoring technology for hazardous gases remains underdeveloped, highlighting the urgent need for advancements in real-time online detection of hazardous gases in natural gas transmission.

With the advancement of artificial intelligence technology, the use of infrared spectroscopy for online monitoring of hazardous gases in the natural gas transmission process has become feasible [5-10]. By integrating deep learning [11-15], this study investigates the online monitoring technology for hazardous gases in natural gas pipelines using the GoogLeNet model and proposes a symmetric point-based GoogLeNet infrared spectroscopy monitoring technique.

Through theoretical and experimental analysis, considering all performance evaluation metrics, it is evident that GoogLeNet has significant advantages in detecting hazardous gases during natural gas transmission. After expanding the dataset and retraining the GoogLeNet model, its performance is further enhanced, ensuring that it meets the fundamental requirements for hazardous gas detection in the natural gas transmission process.

ISSN:3007-9640 DOI: https://doi.org/10.70114/acmsr.2025.3.1.P56

2. The Principle of Infrared Spectroscopy for Hazardous Gas Detection

Hazardous gas infrared spectroscopy detection utilizes the principles of infrared spectroscopy and energy levels to detect hazardous gases in natural gas pipelines.

Infrared Spectroscopy Detection Principle: A beam of infrared light with a continuous wavelength is emitted and passed through the substance being measured. When the motion frequency of a specific molecular component in the substance matches the frequency of the infrared light, the molecule absorbs the infrared energy, transitioning from its original ground energy level to a higher energy level. At this moment, the molecule undergoes vibrational and rotational energy level transitions, and the infrared light at the corresponding wavelength is absorbed by the substance. According to quantum mechanics theory:

$$E_n = \left(n + \frac{1}{2}\right) hv \tag{1}$$

In the equation: h is Planck's constant, v is the vibration frequency, and n is the vibrational quantum number.

During the detection process, when the energy of an infrared photon matches the energy difference between molecular energy levels, the infrared light irradiating the detected molecular group is absorbed, causing the molecule to transition to an excited state. This results in an increase in the vibration amplitude of the molecule. Therefore, infrared spectroscopy detection is essentially a method for identifying and distinguishing different compounds based on the relative vibrations between atoms within a molecule and molecular rotation.

The design scheme of the hazardous gas detection platform for natural gas pipelines is shown in Figure 1. It primarily includes a gas collection control cabinet, an infrared spectrometer, a chromatography signal acquisition unit, and a host computer. The monitoring and control host computer incorporates an embedded system for image processing, execution of deep learning programs, and output of recognition results. This system offers high stability and strong anti-interference capability, allowing it to adapt to the harsh working environment of coal mines. The support structure is made of I-beams to provide stable support for each component, preventing unnecessary vibrations during the detection process and minimizing errors.

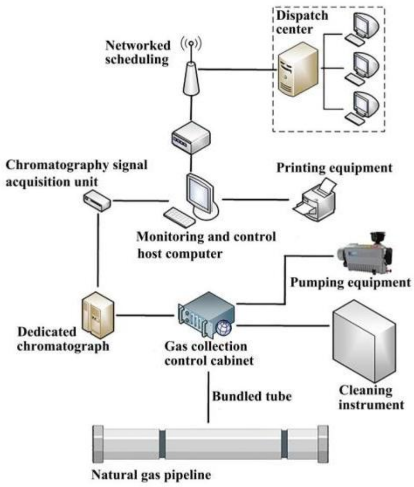

Fig.1 Block diagram of the detection system platform

As shown in Figure 1, the collected image data is encoded and transmitted to the embedded system through the acquisition unit. In the embedded host, the images are processed using a deep learning network for real-time detection of hazardous gases in natural gas pipelines. The results are then transmitted to the fan monitoring room, providing feedback on the presence of hazardous gases during the natural gas transmission process.

ISSN:3007-9640 DOI: https://doi.org/10.70114/acmsr.2025.3.1.P56

3. GoogLeNet Infrared Spectroscopy Detection Based on Symmetric Point Mode

3.1 Symmetric Point Mode Principle

For the acquired spectral signal s, let s_k be the amplitude of the k-th sampling point in signal s, and s_{k+1} be the amplitude of the $k+1$-th sampling point after a time delay l. The signal s can be transformed into a pair of symmetric points $M(R,Z,Y)$ in the polar coordinate system using the symmetric point mode, where R is the radial distance, and Z and Y represent the left and right angles in the polar coordinate diagram, respectively. The calculation formulas for R, Z, and Y are as follows:

$$\mathrm{R} = \frac{s_k - s_{min}}{s_{max} - s_{min}} \tag{2}$$

$$\mathrm{Z} = \frac{360°}{a} + \frac{s_{k+l} - s_{min}}{s_{max} - s_{min}} g \tag{3}$$

$$\mathrm{Y} = \frac{360°}{a} - \frac{s_{k+l} - s_{min}}{s_{max} - s_{min}} g \tag{4}$$

In the equation: s_{max} is the maximum value of the original data of the detected hazardous gas; s_{min} is the minimum value of the original data of the detected hazardous gas; g is the gain of the polar coordinate diagram; l is the time delay; 360°/a represents the initial angle rotation, where parameter a typically determines the number of "petals" in the transformed pattern. To obtain a hexagonal snowflake shape, this paper sets the parameter a to 6.

3.2 GoogLeNet Transfer Learning

The essential feature of the GoogLeNet network is the introduction of the Inception network topology, which approximates the optimal local sparse solution using dense components.

To mitigate the issue of an explosive increase in network parameters, certain adjustments have been made to the existing Inception structure. The most significant modification is the addition of a 1×1 convolution layer after the 3×3 and 5×5 convolution layers, as well as the max pooling layer, to refine the structure and perform dimensionality reduction. Finally, at the output stage, feature concatenation is performed using boundary alignment with thickness as the axis. This approach reduces the number of parameters in this part of the network by a factor of four compared to the previous structure.

Through these improvements and adjustments, a new Inception structure is obtained. The overall loss calculation formula for the GoogLeNet network is as follows:

$$\mathrm{L_z} = 0.3 \cdot \mathrm{softmax0} + 0.3 \cdot \mathrm{softmax1} + \mathrm{softmax2} \tag{5}$$

After the second max pooling, the network enters the Inception structure, where the input feature map has a size of 28×28×192. Each Inception structure consists of four independent branch structures, and these four branches extract features of different scales from the sample through various convolution operations. Finally, the feature maps from the four branches are concatenated, resulting in a final feature map of size 28×28×(64+128+32+32) = 28×28×256.

In the transfer learning process, first, all network parameters before the fully connected layer are frozen, and the pre-trained network parameters obtained from the large-scale ImageNet dataset are directly transferred to the layers before the fully connected layer. Then, a new fully connected layer is constructed for logistic regression. Finally, as before, the samples are classified using the Softmax layer. The structure of the transfer learning model is shown in Figure 2.

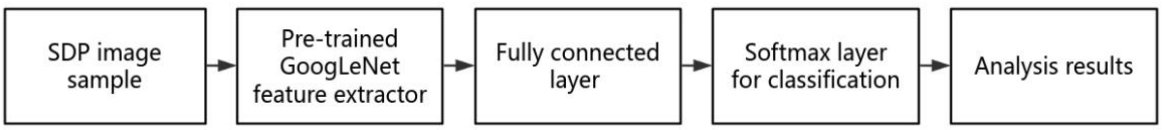

Fig.2 Transfer learning model structure

ISSN:3007-9640 DOI: https://doi.org/10.70114/acmsr.2025.3.1.P56

Constructing a new fully connected layer for network concatenation, the core is to map the n-dimensional real-valued features to K (where K is the number of classification categories) n-dimensional real-valued spaces. The result obtained after the mapping is the score representing the likelihood of the input sample belonging to a specific category. Here, linear logits regression is used to build the fully connected layer, and the relevant calculation formula is:

$$z_k = w_j^T \cdot x \tag{6}$$

In the equation: x is the input vector of the sample; w is the parameter weight matrix.

The Softmax layer for classification maps M values from the real number domain to a (0,1) distribution, thereby obtaining M probability values within the (0,1) interval. These values represent the probabilities that the sample belongs to a specific class in the final classification result. Clearly, the sum of these probability values after mapping is 1. The Softmax mapping function is:

$$\hat{y} = \mathrm{softmax}(z) = \mathrm{softmax}(W^T x + b) \tag{7}$$

Using the pre-trained GoogLeNet feature extractor, the feature vector of the input sample data is extracted. Then, through the classification layer, the feature vector is mapped to obtain the class probabilities, which are used to determine the final class to which the input sample belongs. The higher the final probability score, the higher the confidence in the identified result. The specific process of GoogLeNet feature mapping and recognition is shown in Figure 3.

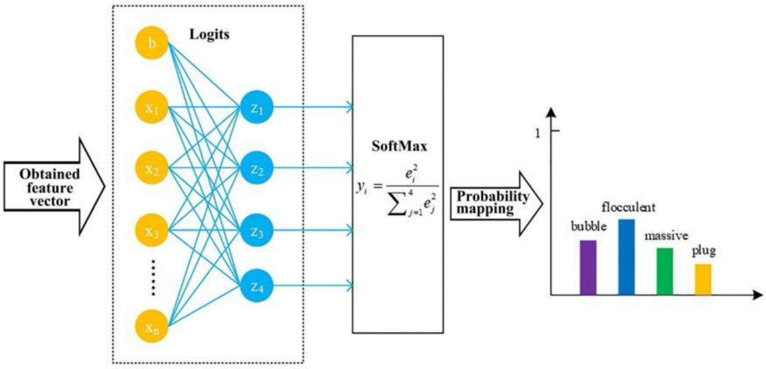

Fig.3 Transfer learning network mapping process

As shown in Figure 2, the collected image data is encoded and transmitted to the embedded system through the acquisition unit. In the embedded host, the images are processed using a deep learning network for real-time detection of hazardous gases in natural gas pipelines. The results are then transmitted to the fan monitoring room, providing feedback on the presence of hazardous gases during the natural gas transmission process.

4. Case Example

4.1 SDP Parameter Analysis

The CO2, CH4, and C2H6 infrared spectral data collected are used to verify the feasibility of the SDP method in processing time-series signals. The spectral data were obtained using a DOW KBr front prism, with a data dimension of 716. Figure 4 shows the infrared spectral images of CO2, CH4, and C2H6.As seen in Figure 4, the spectral curves of the three gases overlap, which is detrimental to the analysis of the spectral data. Therefore, the spectral data can first be converted using the SDP method to obtain the transformed images, which are then analyzed.

ISSN:3007-9640 DOI: https://doi.org/10.70114/acmsr.2025.3.1.P56

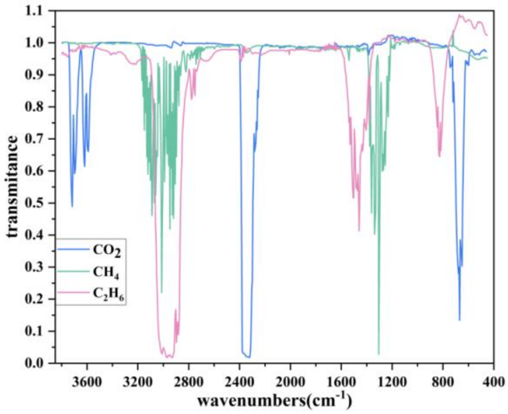

Fig.4 Infrared spectral data of CO2, CH4, and C2H6

There are two parameters that can be optimized in the SDP transformation process: angle amplification gain g and value interval coefficient l. These two parameters together determine the shape and structure of the transformed image. Therefore, the selection of appropriate parameters is crucial for the feature extraction capability of the transformed image, and the most suitable parameters are referred to as dominant parameters. Due to the differences in tasks, the selection of parameters varies accordingly. This paper does not discuss how to select the parameters. A common method is to exhaustively search for the most suitable parameters without affecting the integrity of the data dimension.

4.2 Sample Dataset Construction and Network Training

In the experiment, a total of 1,056 raw sample data images were collected from various scenes with high generalization for hazardous gases. By using the aforementioned method, the sample dataset size was expanded to 2,000 images. The K-fold cross-validation method was used to divide the expanded sample dataset into training, testing, and validation sets.

The specific operation method of K-fold cross-validation is as follows: First, all samples of each class are divided into K subsets of equal size. Then, according to the sequence, the data from the K subsets are selected. The first subset is used as the validation set, the second subset as the test set, and the remaining data as the training set. The network model is trained, and the performance of the results is validated. This process is repeated until all subsets have been used as validation and test sets. Finally, the arithmetic mean of all the performance validation results is calculated, and the obtained result is used as the final evaluation. In the experiment conducted in this paper, K is set to 10, meaning 10-fold cross-validation.

Based on the design of the GoogLeNet harmful gas recognition model using ImageNet transfer learning, the entire network model is trained using the newly constructed dataset. During the training process, since the parameters of the front-end model are already frozen, only the parameters of the redefined fully connected layer and classification layer need to be optimized. When external samples arrive at the network input, features are selected through the established feature extractor and then processed step by step.

After 100 iterations of training the GoogLeNet-based harmful gas recognition model, the highest accuracy reached 97.59%, and the lowest loss function value was 0.22. Testing the obtained network parameters showed that the network has excellent generalization ability, and the overall evaluation results were quite satisfactory. The specific training accuracy and loss function variation curves during the network model training are shown in Figure 5.

ISSN:3007-9640 DOI: https://doi.org/10.70114/acmsr.2025.3.1.P56

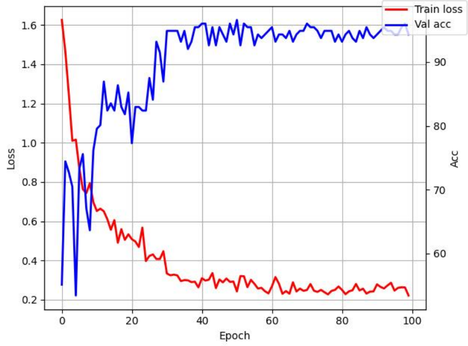

Fig.5 The accuracy and loss function variation curves during the network model training process

4.3 Experiment

For the task of harmful gas recognition in the natural gas transportation process, the performance of five network models was compared using comprehensive metrics. The comparison results are shown in Table 1.

Tab. 1 Performance comparison results

Network model	Validation set size	Accuracy/%	Running time/s	mAP/s
GoogLeNet	200	97.59	8.44	0.042
ResNet	200	86.87	13.10	0.065
VGGNet	200	93.13	19.75	0.099
DenseNet	200	93.18	25.42	0.127
MobileNet	200	97.16	7.25	0.036

Through experimental testing and comprehensive comparison of the performance metrics of the five network models, it is observed that, with the same number of validation samples, there is a significant difference in the models' running times. Among them, MobileNet has the fastest prediction speed, requiring only 7.25 seconds to complete detection for 200 samples. Next is GoogLeNet, with a time of approximately 8.44 seconds, while the remaining three network models have relatively longer running times: 13.10 seconds, 19.75 seconds, and 25.42 seconds, respectively. This indicates that the other three network models require higher computational power to complete predictions, making their application in embedded devices more challenging.

In terms of prediction time for a single sample, the mAP values of the four network models—GoogLeNet, ResNet, VGGNet, and MobileNet are all within 0.1 seconds, indicating relatively ideal detection speeds for single samples. As for the Accuracy of the five network models, GoogLeNet achieves the highest accuracy at 97.59%, followed by MobileNet with 97.16%. The other three network models have Accuracy values below 95%, which indicates that these models perform poorly for the task of harmful gas detection in underground environments.

5. Conclusions

This paper is based on the principle of infrared spectroscopy to detect harmful gases in the natural gas transmission process and designs a detection platform for harmful gases in the natural gas transmission process. Combined with deep learning, the GoogLeNet model is used to analyze harmful gases in the natural gas transmission process, and a symmetric-point GoogLeNet infrared spectroscopy harmful gas monitoring scheme for the natural gas transmission process is proposed.

Experimental research was conducted on CO2, CH4, and C2H6 gases. Through the analysis of infrared spectral data of the three gases and the application of the SDP principle to transform the spectral data, 2000 samples were analyzed. The GoogLeNet model achieved a detection accuracy of 97.59% with a runtime of 8.44s. The results comprehensively demonstrate that the symmetric-point

ISSN:3007-9640 DOI: https://doi.org/10.70114/acmsr.2025.3.1.P56
GoogLeNet model has significant advantages and can effectively complete the task of detecting harmful gases in the natural gas transmission process based on infrared spectroscopy principles.

Acknowledgements

This research is supported by "Monitoring and Sensing System for Safe and Efficient Operation of Cross-regional Complex Oil and Gas Pipeline Network and Its Application (2022YFB3207600)".

References

[1] Wang Zhenhong, Hou Xiongfei, Bian Ming, et al. Safety criterion for impacts of bursting on long-distance gas pipeline[J]. Oil & Gas Storage and Transportation, 2016, 35(08): 813-818.

[2] Tan Lianchu. Analysis of Hazardous Factors in the Integration of Gas Pipelines into Urban Utility Tunnels[J]. China Metal Bulletin, 2017, (07): 166-167.

[3] Fan Wenfeng, Fan Jiwen, Pang Zhihui, et al. Impact of Pile Foundation Construction on Buried Natural Gas Pipelines and Control Measures[J]. Gas & Heat, 2018, 38(05): 80-84.

[4] Liu Bo. Analysis of Hazardous Factors and Safety Technical Measures in Natural Gas Pipeline Engineering Construction[J]. China Petroleum and Chemical Standard and Quality, 2021, 41(08): 72-73.

[5] Zhang Yunhao, Yang Yunpeng, Sun Bingcai, et al. Infrared spectroscopic imaging detection components for oil and gas leak detection[J]. Infrared and Laser Engineering, 2025, 54(2): 20240316.

[6] Cao Jiangtao, Li Quancheng, Ban Ming, et al. Review of hazardous gas detection technology based on infrared spectral imaging [J]. Science Technology and Engineering, 2023, 23(19): 8050-8060.

[7] Qu Guangming, Yang Yingli, Wang Guodong, et al. Research progress in properties modification of metal oxide semiconductor gas sensors[J]. Transducer and Microsystem Technologies, 2022, 41(2):1-4.

[8] Zhu Pengcheng, Liu Haoran, Ji Xiangguang, et al. Study on Measurement of Tropospheric NO2 in Beijing by MAX-DOAS[J]. Spectroscopy and Spectral Analysis, 2021, 41(7): 2153-2158.

[9] Zhang Qiuying, Jin Xuesong. Flower image classification based on convolutional neural network and transfer learning[J]. Journal of Harbin University of Commerce (Natural Sciences Edition), 2020, 36(3): 323-327.

[10] Deng Xiangwu, Ma Xu, Qi Long, et al. Recognition of Rice Field Seedling-Stage Weeds Based on Convolutional Neural Networks and Transfer Learning[J]. Journal of Agricultural Mechanization Research, 2021, 43(10): 167-171.

[11] Li Sining. Research on Facial Micro-expression Recognition Methods Based on Deep Learning[D]. China University of Mining and Technology, 2020.

[12] Chang Jingfei, Lu Yang, Xue Ping, et al. Iterative clustering pruning for convolutional neural networks[J]. Knowledge-based Systems, 2023: 265-272.

[13] Jaswal R A, Dhingra S. Empirical analysis of multiple modalities for emotion recognition using convolutional neural network[J]. Measurement: Sensors, 2023: 26.

[14] Li Ying, Song Lijuan. Research on Remote Sensing Image Recognition and Classification Based on GoogLeNet Model[J].Computer Knowledge and Technology, 2021, 17(12): 4-6.

[15] Wang Yue, Jin Yinggu, Li Yang, et al.Bark image recognition method based on GoogLeNet[J].Modern computer, 2021(22): 128-132.